Chapter 4

Controlled Porosity in Thermochromic Coatings

Ning Wang, Yujie Ke and Yi Long

Additional information is available at the end of the chapter

http://dx.doi.org/10.5772/intechopen.70890

Abstract

Vanadium dioxide is a promising thermochromic material, seemed as the great candidate for smart window applications. The real application of VO_2 requires high visible transmission (T_{lum}) as well as large solar modulating abilities (ΔT_{sol}), which could not be achieved by pristine VO_2 materials due to the trade-off between T_{lum} and ΔT_{sol}. Here in, the porosity design is thoroughly reviewed from the effect on modulating the thermochromic performance to the porous control and preparation. To begin with, the history, advantages, challenges and approaches to tackle the issues comprised of anti-reflection multilayer structure, nanothermochromism, patterning and porous design is introduced in detail. Then, the effect of porosity on improving the thermochromic performance of VO_2 thin films is demonstrated using the newest experimental and simulation results. In the following, the porous control and structural synthesis, including the polymer-assisted deposition (PAD), freeze-drying, colloidal lithography as well as the dual phase transformation is summarized. Fourthly, the characterization methods, composed of scanning electron microscopy (SEM), transmission electron microscopy (TEM), atomic force microscopy (AFM), X-ray diffraction (XRD), Raman spectroscopy as well as UV-Vis-NIR spectroscopy are demonstrated. Finally, the challenges that the porous design faces and possible approaches to optimize the performance are presented.

Keywords: porosity, vanadium dioxide, thermochromism, smart window, energy saving

1. Introduction

In recent decades, the usage of traditional energy materials, including the oil and the coal meets more and more challenges due to the increase of air pollution, energy shortage and the global warming. Therefore, the concepts of sustainable and environment-friendly production were raised by scientists for energy-saving, and various clean energy technologies have been proposed for industries, for example, fuel cell [1–4], solar cell [5–7] and wind turbines [8–11].

On the other hand, the alternative energy-saving approach is to develop green-energy buildings equipped with state-of-the-art smart windows, for example, electrochromic/thermochromic smart windows [12–17].

Vanadium dioxide (VO_2), as a promising coating material for thermochromic smart windows have been investigated for half a century, since Morin found the intrinsic metal-to-insulator transition (MIT) of VO_2 in 1959 [18]. Below a critical temperature (τ_c) ~ 68°C, VO_2 shows the monoclinic insulating phase (VO_2(M)) with zig-zag V-V chains along the *c*-axis ($P2_1$/c, V-V separation is 0.262, 0.316 nm) [19]. Above the τ_c, VO_2 is transformed to rutile metallic phase (VO_2(R)) with linear V-V chains along the *c*-axis ($P4_2$/mnnm, V-V separation is 0.288 nm) [19]. The increase of the electrical resistance across the MIT is always in 3–5 orders of magnitude, and the first-order transition could occur simultaneously with the time less than 500 fs [20]. Along with the MIT, the IR transmittance of VO_2 could also be modulated by a large magnitude owing to the change of the optical parameters (refractive 'n' and extinction coefficient 'k') [21]. As a coating material, VO_2 shows the high IR transmittance at the cold state while exhibits the large absorption as well as the strong reflection at the hot state, which gives rise to large IR modulating ability [22–25]. Due to the little difference of optical parameters in the visible region, VO_2 shows the little transmittance difference in the visible region [26–28]. The solar modulating ability especially in the IR region makes VO_2 a promising coating material for thermochromic smart windows.

The VO_2 thermochromic smart windows have various advantages in energy saving. To begin with, the phase transition temperature (τ_c) of VO_2 is close to the room temperature, which cannot be found in other phase transition materials ($\tau_c(V_2O_3)$ = −123°C, $\tau_c(V_2O_5)$ = 257°C, $\tau_c(V_6O_{13})$ = −123°C, $\tau_c(Ti_nO_{2n+1})$ = 127–377°C) [27]. Secondly, the τ_c of VO_2 could be further reduced to ambient temperature through doping with other high valence metal cations, for example, W^{6+} [22, 29–33], Mo^{6+} [34–36]. Finally, several synthetic methods, for example, atmospheric pressure CVD [36–40], magnetron sputtering [41–45], sol-gel [35, 46, 47] and hydrothermal assembly [48–50], have been developed to fabricate VO_2 nanostructures for applications. However, for thermochromic applications, VO_2 still meets several challenges. Firstly, it is hard to achieve the high visible transmittance (T_{lum}) and the large solar modulating abilities (ΔT_{sol}) simultaneously, since there is always a tradeoff between the T_{lum} and ΔT_{sol} [51]. Secondly, the thermochromic property is hard to maintain when reducing the τ_c to room temperatures via doping [31]. Finally, the VO_2 coating is not stable in the air [52].

In order to improve the thermochromic performance of VO_2 coating, several interesting strategies, including nanoporosity, nanothermochromism, patterning as well as multilayer structures have been investigated by the scientists. Gao's group reported the enhanced luminous transmittance (T_{lum} = ~40%) and improved thermochromic properties (ΔT_{sol} = ~14%) of nanoporous VO_2 thin films with low optical constants, and the optical calculations suggested that the further improved performance could be expected by increasing the thin film porosity [53]. Li et al. [54] calculated the nanothermochromics of VO_2 nanocomposite by dispersing VO_2 nanoparticles in the dielectric host, which revealed that the thermochromic performance could be largely enhanced (T_{lum} = ~65%, ΔT_{sol} = ~20%) with spherical morphologies of the VO_2

nanoparticles in the nanocomposite. Long's group investigated the micropatterning [55] and nanopatterning [51] of VO_2 thin films, which both benefited the VO_2 thin films with improved T_{lum} and ΔT_{sol}. Mlyuka et al. reported the five-layer $TiO_2/VO_2/TiO_2/VO_2/TiO_2$ structure, which showed the high T_{lum} (~43%) and the large ΔT_{sol} (~12%). Across the strategies, the nanoporous design showed the advantages in easy-to-handling, low usage of VO_2 materials as well as the thickness control.

2. Enhanced thermochromic properties of VO_2 with porous structure

As is well known, the porous structure could effectively increase the specific area of materials and thus supply large active areas under low loading. On the other hand, the porous design could also reduce the optical constants (refractive index 'n' and the extinction coefficient 'k'), which could benefit the materials with enhanced visible transmittance. The optical calculations of nanoporous VO_2 thin films could be performed with an optical-admittance recursive method, based on the assumption that the optical constants should be linearly dependent on the volume fraction or the 'n' and 'k' is linearly decreased with the porosity. As shown in **Figure 1**, as for the random distributed nanoporous VO_2 thin films (**Figure 1a**), the porous structure gave rise to an obvious decrease of optical constants (n, k) compared with the normal thin film, and the optical calculations revealed the largely enhanced T_{lum} and ΔT_{sol} with increasing the porosity of the thin films.

With respect to the porous structure of VO_2 thin films, there are normally the random distributed and the periodic porous structures. In the random case, as reported by Gao's group [53] and Long's group [57], the thermochromic properties could be enhanced to $T_{lum} > 40\%$ and $\Delta T_{sol} > 14\%$. In contrast, for the periodic porous structure, as reported by Xie's group [58] and further developed by Long's group [59, 60], the visible transmittance could be above 46% while maintaining the ΔT_{sol} above 13%. Actually, the periodic nanoporous design is more

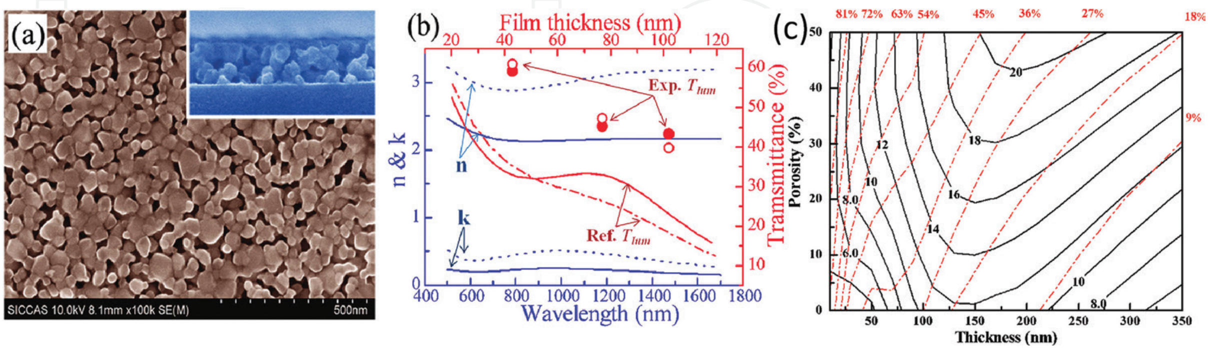

Figure 1. (a) Nanoporous VO_2 thin film. (b) Experimental (solid) and reference (dash) n, k (versus wavelength) and experimental/reference T_{lum} (versus film thickness). Reference data is from Jin et al. [56]. (c) Optical calculations of the nanoporous VO_2 thin films based on an optical-admittance recursive method, where dotted lines and solid lines represent the T_{lum} at insulating state and the ΔT_{sol}, respectively [53].

efficient in controlling the porosity and optimizing the thermochromic properties than the random counterpart, since the porosity could be easily estimated from the structure design.

3. Porous control and synthetic methods

In the nanoporous design for thermochromic VO_2 thin films, there are mainly four different approaches to synthesize and control the porosity, including the polymer assistant deposition (PAD) [53], freeze-drying preparation [57], colloidal lithography assembly [58] as well as the dual-phase transformation [61].

To begin with the PAD, it is a powerful technique to get the continuous nanoporous VO_2 thin films. The polymer used in the PAD process could be cetyltrimethyl ammonium bromide (CTAB) [62], cetyltrimethylammonium vanadate (CTAV) [63], polyvinylpyrrolidone (PVP) [53, 64, 65] or polyethylenimine (PEI) [66, 67]. Take CTAB as an example, when the vanadium precursor was modified by the amphiphilic polymer, the nuclear could be effectively isolated and the nanopores could be formed during the annealing process (**Figure 2**) [62]. It should be noted that the control of the polymer addition is critical to optimize the shape and size of the nanopores.

Freeze-drying is also an efficient way to prepare the nanoporous VO_2 thin films. For a normal sol-gel process, it is hard to get a film with high porosity. When the precursor is frozen and then dried in vacuum, the solvents could sublime and be removed quickly from the structure, which therefore gives rise to the in-situ formation of nanoporous structure (**Figure 3d**). In a typical process for fabricating nanoporous VO_2 thin films with freeze-drying, the V_2O_5-H_2O_2-ox (oxalic acid) precursor was firstly dip coated onto fused silica substrates for gelation, and then a pre-freezing process was performed with a following freeze-drying at −80°C and 0.01 mbar [57]. After a post-annealing process under Ar atmosphere at 550°C for 2 h, the nanoporous VO_2 thin films were subsequently obtained (**Figure 3a–c**).

Colloidal lithography assembly is an alternative approach to get the nanoporous VO_2 thin films, especially for the periodic porous design. The close packed monolayer colloidal crystal (MCC) template has been the usual sacrificing template for colloidal lithography assembly, which make it a facile way to prepare the periodic nanoporous structure. In a typical colloidal lithography assembly for nanoporous VO_2 thin films, the polystyrene (PS) MCC template was firstly infiltrated by $VOSO_4$ solution, then the infiltration with NH_4HCO_3 solution as precipitator was performed to confirm the coating of vanadium source on the template. Finally, the template was picked up by a clean substrate, and then the periodic nanoporous VO_2 thin films were attained though annealing in nitrogen gas [58]. The nanoporous structure could be further modulated by changing the layer number and/or the concentration of the precursor, which could help to optimize the thermochromic properties of the thin films.

More systematically, colloidal lithography was explored to prepare the two-dimensional patterned VO_2 films with tunable periodicity and diverse nanostructures including nanoparticle, nanonet and nanodome arrays [59]. The fabrication process is more flexible via introducing of the plasma etching (PE) technology and controlling the precursor viscosity. They concluded

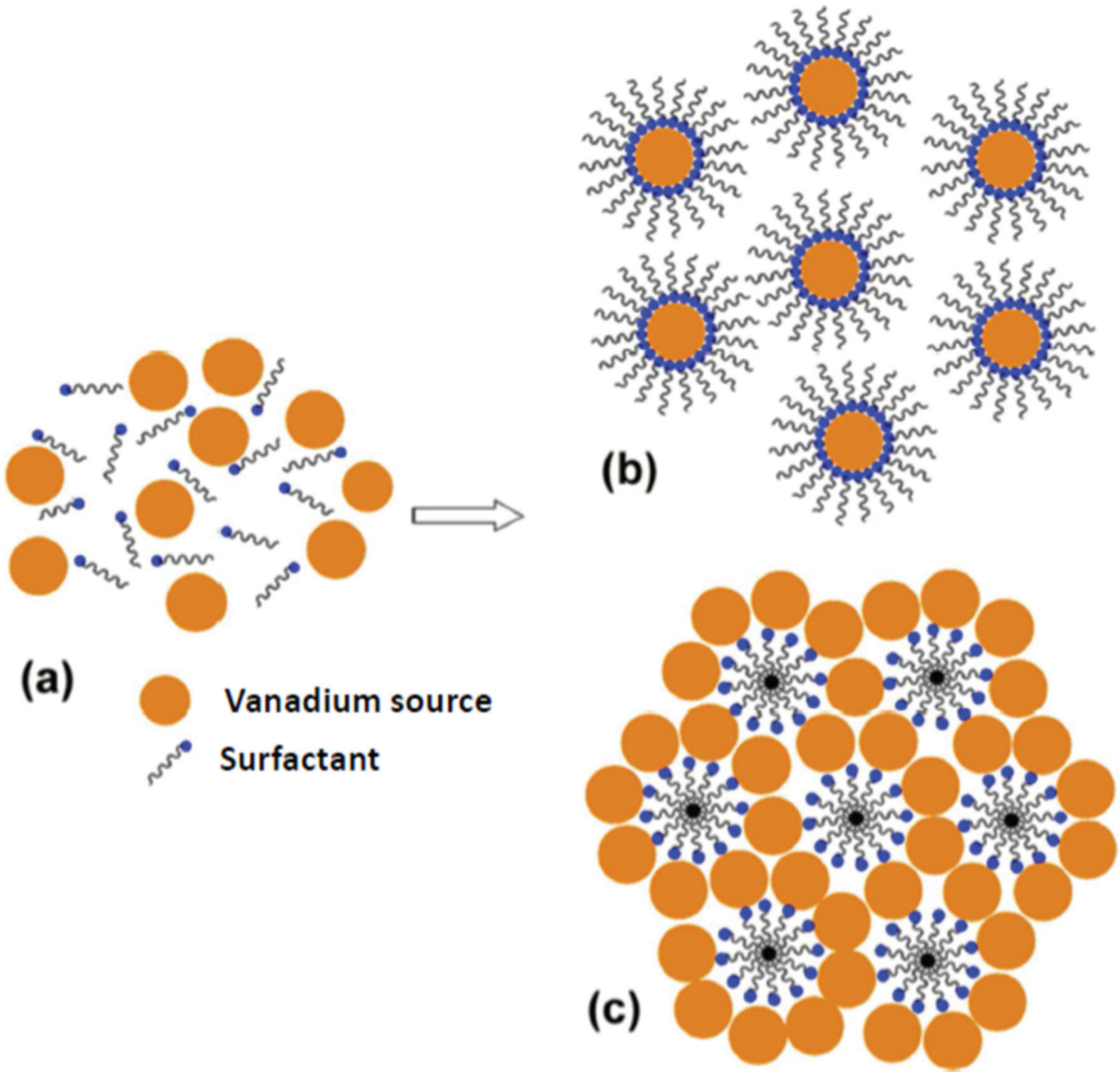

Figure 2. Modification of vanadium precursor by the CTAB. (a) Initial step for adding the CTAB into the vanadium precursor. (b) and (c) Two forms of separation for the nuclear functionalized by the CTAB after strong stirring [62].

the synthesis routes in **Figure 4**. When short PE duration applied, nanoparticle and nanodome arrays are produced using low (Route 1) and high (Route 2) viscosity precursors, respectively. Nanonet arrays are fabricated via prolonging PE duration and using low viscosity precursor (Route 3). Produced two-dimensional patterned VO_2 arrays are highly uniform (**Figure 5**). For the first time, hexagonally patterned VO_2 nanoparticle array with the average diameter down to 60 nm and the periodicity of 160 nm has been fabricated (**Figure 5a**). It is of great interest that such structure gives rise to tunable peak positon and intensity of the localized surface plasmon resonance (LSPR) at different temperature. The LSPR was also found a red-shift with increase of the particle size and the media reflective index, respectively, and these results fit well with the tendency calculated using 3D finite-difference time-domain (FDTD). Besides decent thermochromic performance (up to ΔT_{sol} = 13.2% and T_{lum} = 46%) achieved,

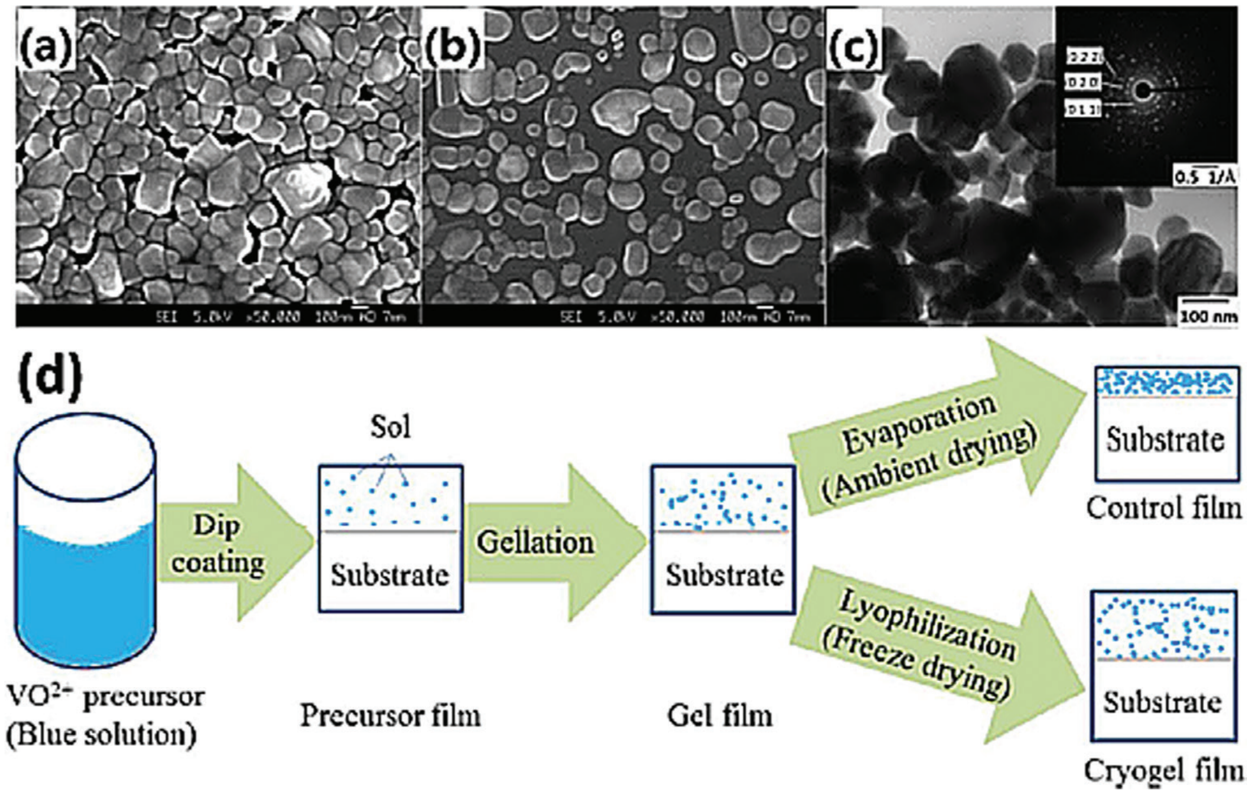

Figure 3. Field-emission scanning electron microscopy (FESEM) image for the freeze-dried nanoporous VO_2 films with 7.5 mL of H_2O_2 (a) and 17.5 mL of H_2O_2 (b) in the precursor. (c) TEM image of (b) and the corresponding SAED (inset). (d) Schematic illustration of the freeze-drying process for the nanoporous design [57].

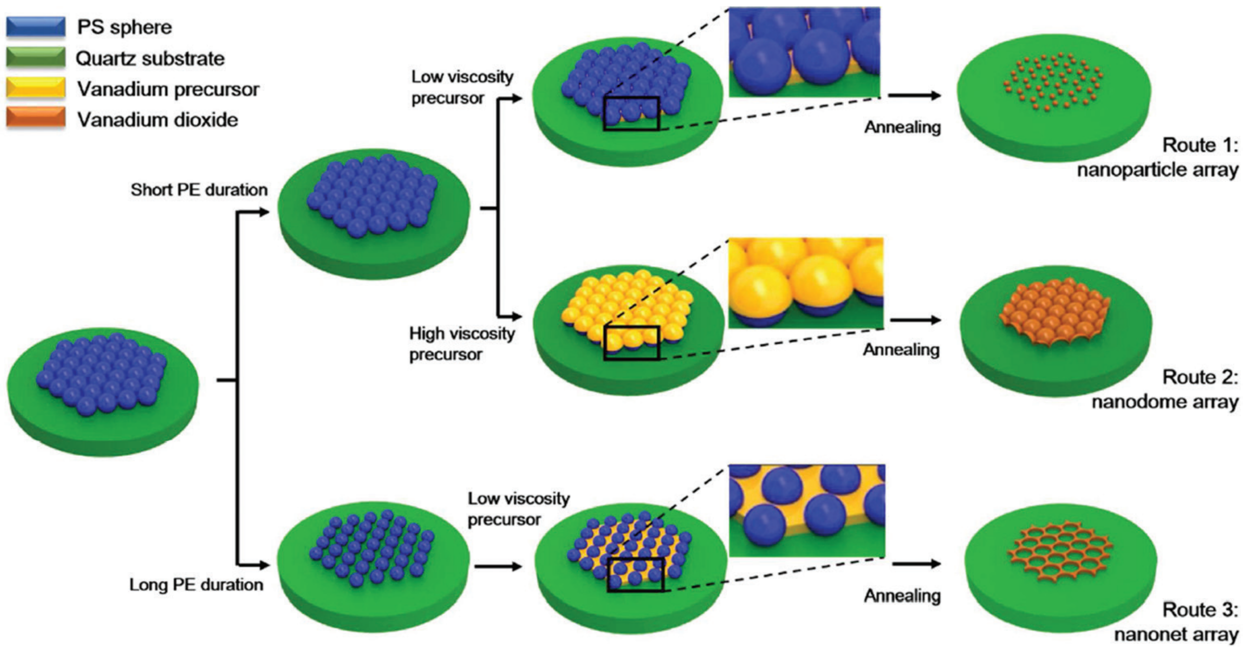

Figure 4. Effect of synthesis conditions on the morphology evolution. Route 1: nanoparticle arrays are prepared via short PE duration and low viscosity precursor; Route 2: nanodome arrays are produced, using high viscosity precursor that can stick on the tops of PS spheres; Route 3, nanonets are fabricated by controlling the interval space between adjacent spheres via long PE duration [59].

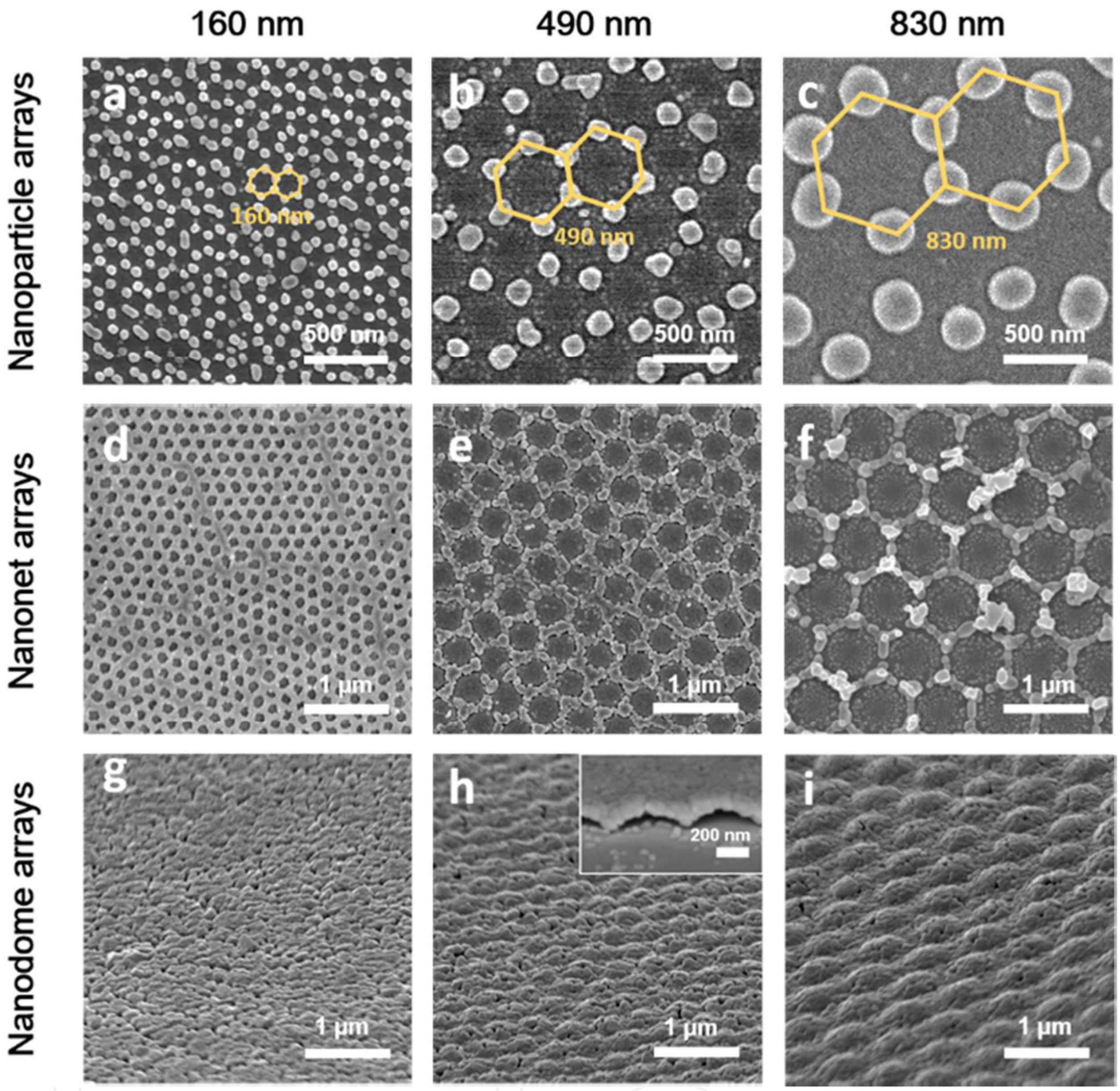

Figure 5. FESEM images of periodic VO_2 films. (a–c) Nanoparticle, (d–f) nanonet, and (g–i) tilted-views of nanodome arrays with periodicity of 160, 490 and 830 nm from left to right, respectively. The insert of (h) is high magnitude tilted-view image of 490 nm periodic nanodome on edge. Yellow hexagons in (a–c) are illustrations for hexagons patterning [59].

the 2D patterned VO_2 films have been demonstrated as an efficient smart thermal radiation filter to remote control the lower critical solution temperature (LCST) behavior of poly N-isopropylacrylamine (PNIPAm) hydrogel. Comparing with template-free method, periodic films produced by nanosphere lithography technique offer more uniform periodicity (less periodic defect) as well as smaller individual nanostructure that is able down to sub-100 nm.

An interesting study using colloidal lithography was to develop photonic structures, consisted of two-dimensional SiO_2-VO_2 core-shell monolayer (**Figure 6a** and **b**) [60]. The structures with periodicity in visible range are demonstrated with the ability to modulate the visible transmittance by selectively reflecting the light with certain color (**Figure 6c**). Benefiting from this ability, smart windows based on such structures display controllable appearances as well as good thermochromic performance, which is up to T_{lum} = 49.6% and ΔT_{sol} = 11.0% calculated by 3D FDTD. This statically visible and dynamically near-infrared modulation is further proved by experiments. However, the optimized thermochromic performance is much lower than that in simulation, which is attributed to the sol-gel method where the perfect core-shell structure cannot be produced in experiment as in simulation. Thus, other more controllable methods, such as physical vapor deposition or chemical vapor deposition, could be proposed as a better way for the fabrication of such two-dimensional core-shell structures.

The dual-phase transformation is a newly developed template-free method to prepare the nanoporous VO_2 thin films with ultrahigh visible transmittance. As depicted in **Figure 7**, this method is based on the transformation between the colloids and ionic states stimulated by the moisture. Firstly, the precursor ($VOCl_2$ + HCl + H_2O + N_2H_4) was spin coated onto fused silica substrates, and then the hydrous colloids were formed through water evaporation. After a quick annealing at 300°C to solidify the film, and an additional annealing at

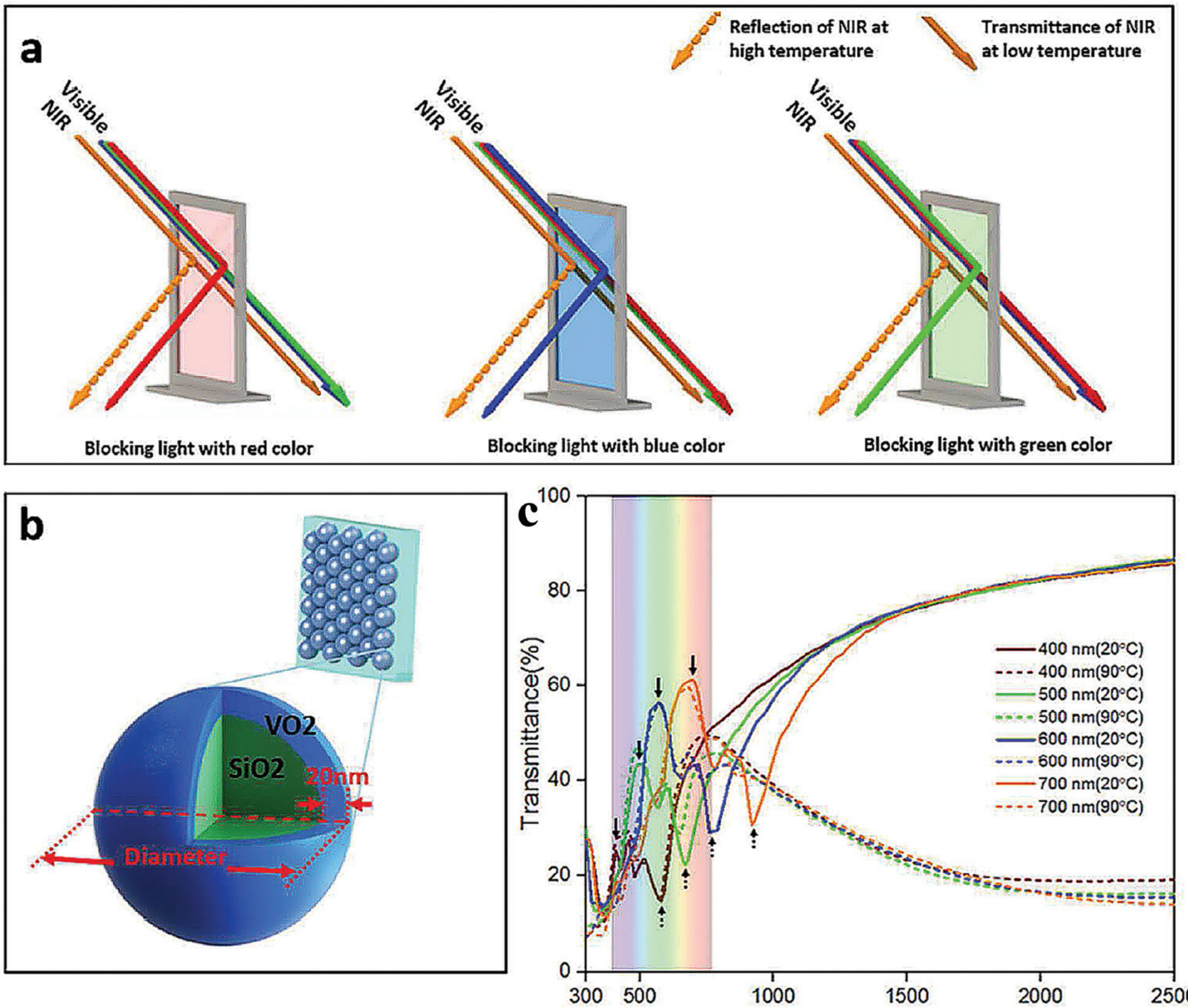

Figure 6. (a) Illustration of how color-changed thermochromic smart window works. (b) Illustration of designed structures for simulation. (c) Calculated transmittance spectrum. The colorful background in (c) denotes the visible spectrum from 370 to 770 nm [60].

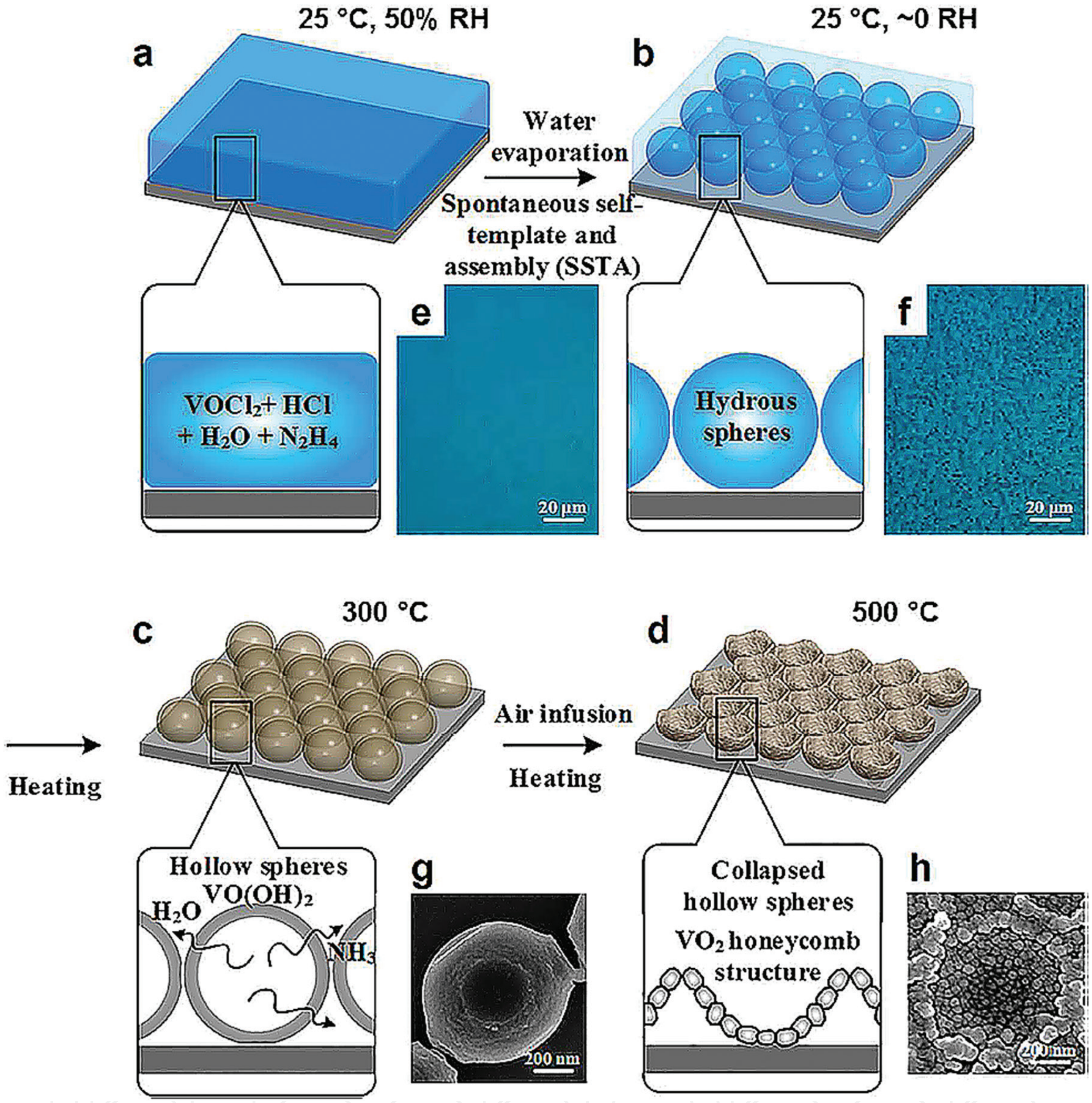

Figure 7. Formation of nanoporous VO_2 thin films through dual phase transformation [61]. (a) Homogeneous, fully solution-based precursor film was deposited at room condition (25 °C, 50% RH). (b) Precursor was spontaneously self-templated and assembled (SSTA) into hydrous sphere arrays after water evaporation in dry nitrogen (25 °C, ~0 RH). (c) Hydrous spheres became hollow $VO(OH)_2$ spheres after instant heating to 300 °C and (d) finally collapsed to honeycomb structures after being heated at a rate of 2 °C and maintained at 500 °C for 1 h. Microscopic photos of (e) the precursor film and (f) the film after SSTA process. SEM images of (g) captured hollow $VO(OH)_2$ spheres and (h) final honeycomb structures.

500°C in N_2, the honeycomb-like nanoporous VO_2 structures were finally obtained with high visible transmittance (~700 nm) above 90% as well as a decent solar modulating ability (ΔT_{sol} = ~5.5%). The critical factor for forming the initial hydrous spheres (colloids) is the ratio control between the HCl and the N_2H_4 [61].

Apart from the above methods, the approaches including, but not limited to the chemical etching [68] and reactive ion etching [69] could also be utilized to produce the VO_2 nanoporous thin films.

4. Characterization

In order to fully characterize the structure and the thermochromic properties of VO_2 nanoporous thin films, the advanced techniques including scanning electron microscopy (SEM), transmission electron microscopy (TEM), atomic force microscopy (AFM), X-ray diffraction (XRD), Raman spectroscopy as well as UV-Vis-NIR spectroscopy could be utilized in the investigation.

With respect to the nanoporous morphology, SEM is a powerful technique to observe the size, shape and the distributions of the nanopores on the surface in a large scale vision, while the details within the pore could be determined using the TEM in a cross-section view. Due to the non-destructive advantage, AFM is also an efficient way to scan the pore distribution on the surface although some artifacts always appear in the AFM images.

Regarding to the thermochromic properties, the VO_2 phase could be firstly confirmed though the XRD and Raman scan, and then the solar modulation ability could be determined with temperature dependent UV-Vis-NIR characterization. As for the XRD, VO_2 (M, $P2_1/c$) will show the crystalline planes (011)/(−211)/(220)/(022)/(202) at the 2θ positions 28°/37°/55.5°/57.5°/65°, while the VO_2 (R, $P4_2/mnm$) will show the crystalline planes (110)/(101)/(211)/(220)/(002) at the 2θ positions 28°/37°/55.5°/57.5°/65° [22, 70]. For the Raman scan [58, 71], the VO_2 (M) phase will show the A_g peaks at the Raman shift positions 192/222/302/392/611 cm^{-1} and the B_g peak at 258 cm^{-1}. In the measurement of thermochromic performance, the transmittance of the normal incidence is recorded at the wavelength range 250–2500 nm at the temperature below and above the τ_c, and the integrated luminous transmission (T_{lum}, 380 nm < λ < 780 nm) and the integrated solar modulating abilities (ΔT_{sol}, 250 nm < λ < 2500 nm) could be calculated from the expression

$$T_{lum/sol} = \int \varphi_{lum/sol}(\lambda) T(\lambda) d\lambda / \int \varphi_{lum/sol}(\lambda) d\lambda \tag{1}$$

where ϕ_{lum} is the standard luminous efficiency function for the photopic vision of human eyes [72], and the ϕ_{sol} is the solar irradiance spectrum for air mass 1.5 (corresponding to the sun standing 37° above the horizon) [73]. ΔT_{sol} is calculated from $T_{sol}(\tau < \tau_c) - T_{sol}(\tau > \tau_c)$.

5. Concluding remarks and outlook

In this chapter, we have elaborated the fabrication of nanoporous VO_2 nanomaterials and the effect of porosity on enhancing the thermochromic properties. Compared with the other property enhancement methods, such as ARC multilayers, biomimetic patterning, nanothermochromism and periodic patterning (**Figure 8**), the porous design shows the advantages in easy-to-handling, low usage of VO_2 materials as well as the thickness control, which could reduce the cost in the real applications. In the fabrication of nanoporous VO_2 thin films, the PAD, freeze-drying as well as the dual-phase transformation are the three main methods for random nanoporous structures, while the colloidal lithography

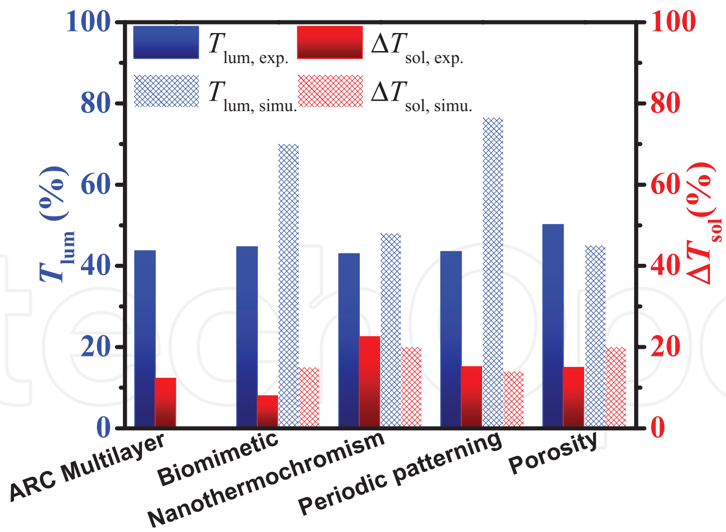

Figure 8. Methods proposed for enhancing the thermochromic performance of VO_2 nanomaterials [55].

with the MCC template is an effective approach for periodic nanoporous structures. The calculations reveal that the nanoporous structure could result in the decrease of optical constants and thus lead to the enhancement of visible transmission while maintain the decent solar modulating abilities.

Although many efforts have been dedicated to optimize the effect of nanoporous structure on enhancing the thermochromic performance of VO_2 thin films, the low visible transmission (<~80%) and the low solar modulating ability (<~30%) restrict the real applications in thermochromic smart windows. From the viewpoint of materials design, the periodic nanoporous VO_2 thin films with the periodicity below 100 nm should give rise to the largely enhanced visible transmission as well as the highly reduced scattering, which could greatly improve the thermochromic performance for smart window applications.

Acknowledgements

This research is supported by National Research Foundation, Prime Minister's Office, Singapore under its Campus for Research Excellence and Technological Enterprise (CREATE) programme.

Author details

Ning Wang, Yujie Ke and Yi Long*

*Address all correspondence to: longyi@ntu.edu.sg

School of Materials Science and Engineering, Nanyang Technological University, Singapore

References

[1] Das V, Padmanaban S, Venkitusamy K, Selvamuthukumaran R, Blaabjerg F, Siano P. Recent advances and challenges of fuel cell based power system architectures and control—A review. Renewable and Sustainable Energy Reviews. 2017;**73**:10-18. DOI: 10.1016/j.rser.2017.01.148

[2] Siebel A, Gorlin Y, Durst J, Proux O, Hasché F, Tromp M, et al. Identification of catalyst structure during the hydrogen oxidation reaction in an operating PEM fuel cell. ACS Catalysis. 2016;**6**(11):7326-7334. DOI: 10.1021/acscatal.6b02157

[3] Macauley N, Watson M, Lauritzen M, Knights S, Wang GG, Kjeang E. Empirical membrane lifetime model for heavy duty fuel cell systems. Journal of Power Sources. 2016;**336**:240-250. DOI: 10.1016/j.jpowsour.2016.10.068

[4] Inukai M, Horike S, Itakura T, Shinozaki R, Ogiwara N, Umeyama D, et al. Encapsulating mobile proton carriers into structural defects in coordination polymer crystals: High anhydrous proton conduction and fuel cell application. Journal of the American Chemical Society. 2016;**138**(27):8505-8511. DOI: 10.1021/jacs.6b03625

[5] Lan X, Voznyy O, Kiani A, García de Arquer FP, Abbas AS, Kim G-H, et al. Passivation using molecular halides increases quantum dot solar cell performance. Advanced Materials. 2016;**28**(2):299-304. DOI: 10.1002/adma.201503657

[6] dos Reis Benatto GA, Roth B, Corazza M, Sondergaard RR, Gevorgyan SA, Jorgensen M, et al. Roll-to-roll printed silver nanowires for increased stability of flexible ITO-free organic solar cell modules. Nanoscale. 2016;**8**(1):318-326. DOI: 10.1039/c5nr07426f

[7] Bi D, Xu B, Gao P, Sun L, Grätzel M, Hagfeldt A. Facile synthesized organic hole transporting material for perovskite solar cell with efficiency of 19.8%. Nano Energy. 2016;**23**:138-144. DOI: 10.1016/j.nanoen.2016.03.020

[8] Song D, Yang J, Dong M, Joo YH. Model predictive control with finite control set for variable-speed wind turbines. Energy. 2017;**126**:564-572. DOI: 10.1016/j.energy.2017.02.149

[9] Pahn T, Rolfes R, Jonkman J. Inverse load calculation procedure for offshore wind turbines and application to a 5-MW wind turbine support structure. Wind Energy. 2017;**20**(7):1171-1186. DOI: 10.1002/we.2088

[10] Tummala A, Velamati RK, Sinha DK, Indraja V, Krishna VH. A review on small scale wind turbines. Renewable and Sustainable Energy Reviews. 2016;**56**:1351-1371. DOI: 10.1016/j.rser.2015.12.027

[11] Shen X, Avital E, Paul G, Rezaienia MA, Wen P, Korakianitis T. Experimental study of surface curvature effects on aerodynamic performance of a low Reynolds number airfoil for use in small wind turbines. Journal of Renewable and Sustainable Energy. 2016;**8**(5):053303. DOI: 10.1063/1.4963236

[12] Zhang P, Zhu F, Wang F, Wang J, Dong R, Zhuang X, et al. Stimulus-responsive micro-supercapacitors with ultrahigh energy density and reversible electrochromic window. Advanced Materials. 2017;**29**(7):1604491. DOI: 10.1002/adma.201604491

[13] Zhou Y, Layani M, Boey FYC, Sokolov I, Magdassi S, Long Y. Electro-thermochromic devices composed of self-assembled transparent electrodes and hydrogels. Advanced Materials Technologies. 2016;**1**(5):1600069. DOI: 10.1002/admt.201600069

[14] Nakano M, Shibuya K, Ogawa N, Hatano T, Kawasaki M, Iwasa Y, et al. Infrared-sensitive electrochromic device based on VO_2. Applied Physics Letters. 2013;**103**(15):153503. DOI: http://dx.doi.org/10.1063/1.4824621

[15] Yang XH, Zhu G, Wang SH, Zhang R, Lin L, Wu WZ, et al. A self-powered electrochromic device driven by a nanogenerator. Energy & Environmental Science. 2012;**5**(11):9462-9466. DOI: 10.1039/c2ee23194h

[16] Granqvist CG, Lansaker PC, Mlyuka NR, Niklasson GA, Avendano E. Progress in chromogenics: New results for electrochromic and thermochromic materials and devices. Solar Energy Materials & Solar Cells. 2009;**93**(12):2032-2039. DOI: 10.1016/j.solmat.2009.02.026

[17] Minkin VI. Photo-, thermo-, solvato-, and electrochromic spiroheterocyclic compounds. Chemical Reviews. 2004;**104**:2751-2776. DOI: 10.1021/cr020088u

[18] Morin F. Oxides which show a metal-to-insulator transition at the Neel temperature. Physical Review Letters. 1959;**3**(1):34-36. DOI: 10.1103/PhysRevLett.3.34

[19] Wu C, Feng F, Xie Y. Design of vanadium oxide structures with controllable electrical properties for energy applications. Chemical Society Reviews. 2013;**42**(12):5157-5183. DOI: 10.1039/c3cs35508j

[20] Petrov GI, Yakovlev VV, Squier JA. Nonlinear optical microscopy analysis of ultrafast phase transformation in vanadium dioxide. Optics Letters. 2002;**27**(8):655-657. DOI: 10.1364/OL.27.000655

[21] Wang N, Goh QS, Lee PL, Magdassi S, Long Y. One-step hydrothermal synthesis of rare earth/W-codoped VO_2 nanoparticles: Reduced phase transition temperature and improved thermochromic properties. Journal of Alloys and Compounds. 2017;**711**:222-228. DOI: 10.1016/j.jallcom.2017.04.012

[22] Wang N, Duchamp M, Xue C, Dunin-Borkowski RE, Liu G, Long Y. Single-crystalline W-doped VO_2 nanobeams with highly reversible electrical and plasmonic responses near room temperature. Advanced Materials Interfaces. 2016;**3**(15):1600164. DOI: 10.1002/admi.201600164

[23] Wang N, Duchamp M, Dunin-Borkowski RE, Liu S, Zeng X, Cao X, et al. Terbium-doped VO_2 thin films: Reduced phase transition temperature and largely enhanced luminous transmittance. Langmuir. 2016;**32**(3):759-764. DOI: 10.1021/acs.langmuir.5b04212

[24] Wang N, Chew Shun NT, Duchamp M, Dunin-Borkowski RE, Li Z, Long Y. Effect of lanthanum doping on modulating the thermochromic properties of VO_2 thin films. RSC Advances. 2016;**6**(54):48455-48461. DOI: 10.1039/c6ra09514c

[25] Wang N, Liu S, Zeng XT, Magdassi S, Long Y. Mg/W-codoped vanadium dioxide thin films with enhanced visible transmittance and low phase transition temperature. Journal of Materials Chemistry C. 2015;**3**(26):6771-6777. DOI: 10.1039/c5tc01062d

[26] Wang S, Liu M, Kong L, Long Y, Jiang X, Yu A. Recent progress in VO_2 smart coatings: Strategies to improve the thermochromic properties. Progress in Materials Science. 2016;**81**:1-54. DOI: 10.1016/j.pmatsci.2016.03.001

[27] Kiri P, Hyett G, Binions R. Solid state thermochromic materials. Advanced Materials Letters. 2010;**1**(2):86-105. DOI: 10.5185/amlett.2010.8147

[28] Parkin IP, Manning TD. Intelligent thermochromic windows. Journal of Chemical Education. 2006;**83**(3):393-400. DOI: 10.1021/ed083p393

[29] Hu LT, Tao HZ, Chen GH, Pan RK, Wan MN, Xiong DH, et al. Porous W-doped VO_2 films with simultaneously enhanced visible transparency and thermochromic properties. Journal of Sol-Gel Science and Technology. 2016;**77**(1):85-93. DOI: 10.1007/s10971-015-3832-z

[30] Gonçalves A, Resende J, Marques AC, Pinto JV, Nunes D, Marie A, et al. Smart optically active VO_2 nanostructured layers applied in roof-type ceramic tiles for energy efficiency. Solar Energy Materials & Solar Cells. 2016;**150**:1-9. DOI: 10.1016/j.solmat.2016.02.001

[31] Zhu J, Zhou Y, Wang B, Zheng J, Ji S, Yao H, et al. Vanadium dioxide nanoparticle-based thermochromic smart coating: High luminous transmittance, excellent solar regulation efficiency, and near room temperature phase transition. ACS Applied Materials & Interfaces. 2015;**7**(50):27796-27803. DOI: 10.1021/acsami.5b09011

[32] Asayesh-Ardakani H, Nie A, Marley PM, Zhu Y, Phillips PJ, Singh S, et al. Atomic origins of monoclinic-tetragonal (rutile) phase transition in doped VO_2 nanowires. Nano Letters. 2015;**15**(11):7179-7188. DOI: 10.1021/acs.nanolett.5b03219

[33] Huang Z, Chen C, Lv C, Chen S. Tungsten-doped vanadium dioxide thin films on borosilicate glass for smart window application. Journal of Alloys and Compounds. 2013;**564**(0):158-161. DOI: 10.1016/j.jallcom.2013.02.108

[34] Batista C, Ribeiro RM, Teixeira V. Synthesis and characterization of VO_2-based thermochromic thin films for energy-efficient windows. Nanoscale Research Letters. 2011;**6**(1):301. DOI: 10.1186/1556-276X-6-301

[35] Mai LQ, Hu B, Hu T, Chen W, Gu ED. Electrical property of Mo-doped VO_2 nanowire array film by melting–quenching sol–gel method. The Journal of Physical Chemistry. B. 2006;**110**(39):19083-19086. DOI: 10.1021/jp0642701

[36] Manning TD, Parkin IP, Blackman C, Qureshi U. APCVD of thermochromic vanadium dioxide thin films-solid solutions $V_{2-x}M_xO_2$ (M = Mo, Nb) or composites VO_2: SnO_2. Journal of Materials Chemistry. 2005;**15**(42):4560-4566. DOI: 10.1039/b510552h

[37] Powell MJ, Quesada-Cabrera R, Taylor A, Teixeira D, Papakonstantinou I, Palgrave RG, et al. Intelligent multifunctional VO_2/SiO_2/TiO_2 coatings for self-cleaning, energy-saving window panels. Chemistry of Materials. 2016;**28**(5):1369-1376. DOI: 10.1021/acs.chemmater.5b04419

[38] Drosos C, Vernardou D. Perspectives of energy materials grown by APCVD. Solar Energy Materials & Solar Cells. 2015;**140**:1-8. DOI: 10.1016/j.solmat.2015.03.019

[39] Vernardou D, Louloudakis D, Spanakis E, Katsarakis N, Koudoumas E. Thermochromic amorphous VO_2 coatings grown by APCVD using a single-precursor. Solar Energy Materials & Solar Cells. 2014;**128**:36-40. DOI: 10.1016/j.solmat.2014.04.033

[40] Blackman CS, Piccirillo C, Binions R, Parkin IP. Atmospheric pressure chemical vapour deposition of thermochromic tungsten doped vanadium dioxide thin films for use in architectural glazing. Thin Solid Films. 2009;**517**(16):4565-4570. DOI: 10.1016/j.tsf.2008.12.050

[41] Zheng J, Bao S, Jin P. TiO_2(R)/VO_2(M)/TiO_2(A) multilayer film as smart window: Combination of energy-saving, antifogging and self-cleaning functions. Nano Energy. 2015;**11**:136-145. DOI: 10.1016/j.nanoen.2014.09.023

[42] Yang M, Yang Y, Hong B, Wang L, Luo Z, Li X, et al. Surface-growth-mode-induced strain effects on the metal-insulator transition in epitaxial vanadium dioxide thin films. RSC Advances. 2015;**5**(98):80122-80128. DOI: 10.1039/c5ra13490k

[43] Qian Y, Wenwu L, Jiran L, Zhihua D, Zhigao H, Jian L, et al. Oxygen pressure manipulations on the metal–insulator transition characteristics of highly (0 1 1)-oriented vanadium dioxide films grown by magnetron sputtering. Journal of Physics D: Applied Physics. 2013;**46**(5):055310. DOI: 10.1088/0022-3727/46/5/055310

[44] Ma JW, Xu G, Miao L. Vanadium dioxide thin films deposited on TiO_2 buffer layer for smart thermochromic glazing of windows. In: Li H, Liu YF, Guo M, Zhang R, Du J, editors. Sustainable Development of Urban Environment and Building Material, Pts 1-4. Vol. 374-377. Stafa-Zurich: Trans Tech Publications Ltd; 2012. p. 1365-1368

[45] Huang ZL, Chen SH, Lv CH, Huang Y, Lai JJ. Infrared characteristics of VO_2 thin films for smart window and laser protection applications. Applied Physics Letters. 2012;**101**(19):191905. DOI: 10.1063/1.4766287

[46] Seyfouri MM, Binions R. Sol-gel approaches to thermochromic vanadium dioxide coating for smart glazing application. Solar Energy Materials & Solar Cells. 2017;**159**:52-65. DOI: 10.1016/j.solmat.2016.08.035

[47] Warwick MEA, Binions R. Advances in thermochromic vanadium dioxide films. Journal of Materials Chemistry A. 2014;**2**:3275-3292. DOI: 10.1039/c3ta14124a

[48] Yu W, Li S, Huang C. Phase evolution and crystal growth of VO_2 nanostructures under hydrothermal reactions. RSC Advances. 2016;**6**(9):7113-7120. DOI: 10.1039/c5ra23898f

[49] Zhang J, Jin H, Chen Z, Cao M, Chen P, Dou Y, et al. Self-assembling VO_2 nanonet with high switching performance at wafer-scale. Chemistry of Materials. 2015;**27**(21):7419-7424. DOI: 10.1021/acs.chemmater.5b03314

[50] Powell MJ, Marchand P, Denis CJ, Bear JC, Darr JA, Parkin IP. Direct and continuous synthesis of VO_2 nanoparticles. Nanoscale. 2015;**7**(44):18686-18693. DOI: 10.1039/c5nr04444h

[51] Qian X, Wang N, Li Y, Zhang J, Xu Z, Long Y. Bioinspired multifunctional vanadium dioxide: Improved thermochromism and hydrophobicity. Langmuir. 2014;**30**(35):10766-10771. DOI: 10.1021/la502787q

[52] Gao YF, Wang SB, Luo HJ, Dai L, Cao CX, Liu YL, et al. Enhanced chemical stability of VO_2 nanoparticles by the formation of SiO_2/VO_2 core/shell structures and the application to transparent and flexible VO_2-based composite foils with excellent thermochromic properties for solar heat control. Energy & Environmental Science. 2012;**5**(3):6104-6110. DOI: 10.1039/c2ee02803d

[53] Kang L, Gao Y, Luo H, Chen Z, Du J, Zhang Z. Nanoporous thermochromic VO_2 films with low optical constants, enhanced luminous transmittance and thermochromic properties. ACS Applied Materials & Interfaces. 2011;**3**(2):135-138. DOI: 10.1021/am1011172

[54] Li SY, Niklasson GA, Granqvist CG. Nanothermochromics: Calculations for VO_2 nanoparticles in dielectric hosts show much improved luminous transmittance and solar energy transmittance modulation. Journal of Applied Physics. 2010;**108**(6):063525. DOI: 10.1063/1.3487980

[55] Lu Q, Liu C, Wang N, Magdassi S, Mandler D, Long Y. Periodical micro-patterned VO_2 thermochromic films by mesh printing. Journal of Materials Chemistry C. 2016;**4**:8385-8391. DOI: 10.1039/c6tc02694j

[56] Xu G, Jin P, Tazawa M, Yoshimura K. Tailoring of luminous transmittance upon switching for thermochromic VO_2 films by thickness control. Japanese Journal of Applied Physics. 2004;**43**(1):186-187. DOI: 10.1143/jjap.43.186

[57] Cao X, Wang N, Law JY, Loo SCJ, Magdassi S, Long Y. Nanoporous thermochromic VO_2(M) thin films: Controlled porosity, largely enhanced luminous transmittance and solar modulating ability. Langmuir. 2014;**30**(6):1710-1715. DOI: 10.1021/la404666n

[58] Zhou M, Bao J, Tao M, Zhu R, Lin Y, Zhang X, et al. Periodic porous thermochromic VO_2(M) films with enhanced visible transmittance. Chemical Communications. 2013;**49**(54):6021-6023. DOI: 10.1039/c3cc42112k

[59] Ke Y, Wen X, Zhao D, Che R, Xiong Q, Long Y. Controllable fabrication of two-dimensional patterned VO_2 nanoparticle, nanodome, and nanonet arrays with tunable temperature-dependent localized surface plasmon resonance. ACS Nano. 2017;**11**(7):7542-7551. DOI: 10.1021/acsnano.7b02232

[60] Ke Y, Balin I, Wang N, Lu Q, Yok AIY, White TJ, et al. Two-dimensional, SiO_2/VO_2 photonic crystals with statically visible and dynamically infrared modulated for smart window deployment. ACS Applied Materials & Interfaces. 2016;**8**(48):33112-33120. DOI: 10.1021/acsami.6b12175

[61] Liu M, Su B, Kaneti YV, Chen Z, Tang Y, Yuan Y, et al. Dual-phase transformation: Spontaneous self-template surface-patterning strategy for ultra-transparent VO_2 solar modulating coatings. ACS Nano. 2017;**11**(1):407-415. DOI: 10.1021/acsnano.6b06152

[62] Shi QW, Huang WX, Xu YJ, Zhang YX, Yue F, Qiao S, et al. Synthesis and terahertz transmission properties of nano-porous vanadium dioxide films. Journal of Physics D: Applied Physics. 2012;**45**(38):385302(1)-385302(6). DOI: 10.1088/0022-3727/45/38/385302

[63] Ding S, Liu Z, Li D, Zhao W, Wang Y, Wan D, et al. Tunable assembly of vanadium dioxide nanoparticles to create porous film for energy-saving applications. ACS Applied Materials & Interfaces. 2013;**5**(5):1630-1635. DOI: 10.1021/am3023724

[64] Zhang Z, Gao Y, Luo H, Kang L, Chen Z, Du J, et al. Solution-based fabrication of vanadium dioxide on F:SnO_2 substrates with largely enhanced thermochromism and low-emissivity for energy-saving applications. Energy & Environmental Science. 2011;**4**(10):4290. DOI: 10.1039/c1ee02092g

[65] Du J, Gao Y, Luo H, Kang L, Zhang Z, Chen Z, et al. Significant changes in phase-transition hysteresis for Ti-doped VO_2 films prepared by polymer-assisted deposition. Solar Energy Materials & Solar Cells. 2011;**95**(2):469-475. DOI: 10.1016/j.solmat.2010.08.035

[66] Ji Y, Zhang Y, Gao M, Yuan Z, Xia Y, Jin C, et al. Role of microstructures on the M1-M2 phase transition in epitaxial VO_2 thin films. Scientific Reports. 2014;**4**:4854. DOI: 10.1038/srep04854

[67] Jia QX, McCleskey TM, Burrell AK, Lin Y, Collis GE, Wang H, et al. Polymer-assisted deposition of metal-oxide films. Nature Materials. 2004;**3**(8):529-532. DOI: 10.1038/nmat1163

[68] Huang A, Zhou Y, Li Y, Ji S, Luo H, Jin P. Preparation of $V_xW_{1-x}O_2$(M)@SiO_2 ultrathin nanostructures with high optical performance and optimization for smart windows by etching. Journal of Materials Chemistry A. 2013;**1**(40):12545-12552. DOI: 10.1039/c3ta12232h

[69] Bai J, Wang D, Nam S-w, Peng H, Bruce R, Gignac L, et al. Fabrication of sub-20 nm nanopore arrays in membranes with embedded metal electrodes at wafer scales. Nanoscale. 2014;**6**(15):8900-8906. DOI: 10.1039/c3nr06723h

[70] Wu C, Zhang X, Dai J, Yang J, Wu Z, Wei S, et al. Direct hydrothermal synthesis of monoclinic VO_2(M) single-domain nanorods on large scale displaying magnetocaloric effect. Journal of Materials Chemistry. 2011;**21**(12):4509-4517. DOI: 10.1039/c0jm03078c

[71] Zhang H, Li Q, Shen P, Dong Q, Liu B, Liu R, et al. The structural phase transition process of free-standing monoclinic vanadium dioxide micron-sized rods: Temperature-dependent Raman study. RSC Advances. 2015;**5**(101):83139-83143. DOI: 10.1039/c5ra15947d

[72] Wyszecki G, Stiles WS. Color Science: Concepts and Methods, Quantitative Data and Formulae. 2nd ed. New York: Wiley; 2000

[73] In ASTM G173-03 Standard Tables of Reference Solar Spectral Irradiances: Direct Normal and Hemispherical on a 37° Tilted Surface, Annual Book of ASTM Standards. American Society for Testing and Materials: Philadelphia, PA, USA, 2003; **14**(4)

IntechOpen